doi.org/10.1002/cbdv.202300373 Research Article CHEMISTRY & BIODIVERSITY

www.cb.wiley.com

Natural Geranylated Sulfur-Containing Amides with Inhibitory Effect on Th17 Differentiation

Kai-Long Ji[+],*[a] Yan-Qing Tang[+],[b] Zheng-Yang Guo[+],[b] Pian-Chou GongPan,[a] Peng Sun,[a] Jian-Mei Lu,[a] Meng-Yuan Dai,[c] and Ting Li*[b]

Chemical investigation of medicinal plant *Glycosmis lucida* Wall. ex C. C. Huang leaves led to the production of ten compounds (**1**–**10**), including two previously unreported geranylated sulfur-containing amides (**1** and **2**) and eight known ones (**3**–**10**). Structural characterization was carried out using comprehensive spectroscopic methods including NMR, MS and CD. The inhibitory effects of all isolates on Th17 differentiation were evaluated, of which compounds **1** and **6** significantly inhibited Th17 differentiation with IC_{50} values of 0.36 and 1.30 μM, respectively, while both **1** and **6** failed to bind to retinoic acid-related orphan receptor gamma t (RORγt), suggesting that their inhibition of Th17 differentiation is independent of RORγt.

Introduction

CD4+ T helper (Th) cells play important role in immune responses and the pathogenesis of inflammatory diseases. T helper 17 (Th17), a subset of immune CD4+ T cells, is closely related to a variety of inflammatory-related and autoimmune diseases, including psoriasis, rheumatoid arthritis (RA), multiple sclerosis (MS), systemic lupus erythematosus (SLE), and inflammatory bowel disease (IBD).[1,2] IL-17A is the signature cytokine of Th17, which has a strong pro-inflammatory effect and can cause progressive damage to inflammatory tissues. Besides IL-17A, Th17 cells could produce a variety of other cytokines, including IL-21 and IL-17F, indicating that the pathogenic role of Th17 cells depends not only on IL-17A but also on other Th17-derived cytokines.[3] Therefore, inhibition of Th17 cell differentiation is currently an attractive strategy for the treatment of these inflammatory-related and autoimmune diseases.[4]

Glycosmis genus (Rutaceae family) possessed approximately about 50 species, which were shrubs and small trees and distributed in the regions of Southern and Southeast Asia, and Northeastern Australia.[5] In China, there are about 11 species and 1 variety, most of which, including the leaves and roots, have been traditionally used as folk medicines to treat cancer, eczema, wounds, helminthiasis, and skin diseases, etc.[6] Previous chemical investigations revealed that *Glycosmis* plants were rich in alkaloids, flavonoids, terpenoids, phenolics and sulfur-containing amides,[6] as well as the small group of cyclopeptides.[7,8] *Glycosmis lucida* Wall. ex C. C. Huang, a small tree, is mainly distributed in the Yunnan Province of China[5] and commonly used as an ethnodrug for expelling phlegm to arrest coughing and activating blood circulation to dissipate blood stasis detumescence.[7] The crude extract and essential oil of *G. lucida* leaves were reported to have antifeedant activity against insect pests of stored cereals.[9,10] Previous studies have showed that its leaves possessed the antifeedant chemicals of sulfur-containing amides (SCAs)[9,11] and a cyclopeptide.[7]

To data, there are few of scientific reports on the immunologically active chemicals of *G. lucida*. To seek bioactive agents from medicinal plants,[8] the medicinal leaves of *G. lucida* were collected and chemically investigated. Furthermore, the immunosuppressive activities together with the potential mechanism of action of those isolates were investigated in this study.

Results and Discussion

Structure elucidation

The isolated compounds **1**–**6** (Figure 1) showed the coexistence of two conformers (**a** and **b**) at room temperature (r.t.) during ^{1}H-NMR detection in $CDCl_3$ solvent, of which compounds **1** and **4**–**6** possessed the ratio of about 13:7, and compound **2** have the ratio of about 29:21. By comprehensive analysis of the structural features of compounds **1**–**6**, the co-occurrence of two conformers **a** (*anti*-form) and **b** (*syn*-form) within each compound (Figure 2) was likely resulted from the restricted rotation of the C–N within amide group (*p*-π conjugation)[9,12] and/or the keto-enol tautomerization within amide N-methyl group.[11] The major conformer **a** showed the better resolution in ^{1}H and ^{13}C-NMR detections than those of **b** and was selected for structure elucidation.

[a] *K.-L. Ji,[+] P.-C. GongPan, P. Sun, J.-M. Lu*
CAS Key Laboratory of Tropical Plant Resources and Sustainable Use, Xishuangbanna Tropical Botanical Garden, Chinese Academy of Sciences, Kunming 650223, China
E-mail: kl14ji@163.com

[b] *Y.-Q. Tang,[+] Z.-Y. Guo,[+] T. Li*
State Key Laboratory of Quality Research in Chinese Medicines, Macau Institute for Applied Research in Medicine and Health, Macau University of Science and Technology, Macau 999078, China
E-mail: tli@must.edu.mo

[c] *M.-Y. Dai*
Industrial Crop Research Institute, Yunnan Academy of Agricultural Sciences, Kunming 650223, China

[+] *These authors contributed equally to this work.*

Supporting information for this article is available on the WWW under https://doi.org/10.1002/cbdv.202300373

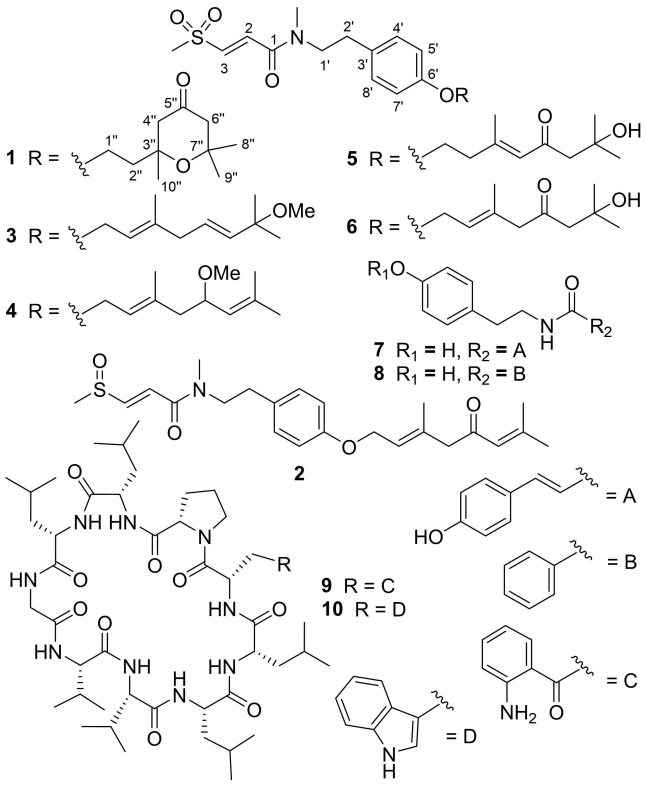

Figure 1. Structures of isolated compounds **1**–**10**.

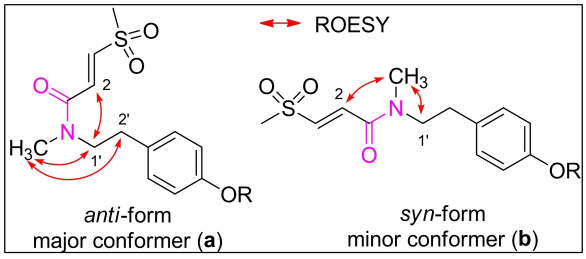

Figure 2. Two conformers of isolated compounds **1**–**6**.

Glylucidamide A (**1**) was obtained as a colorless gum with a molecular formula of $C_{23}H_{34}NO_6S$ by the HR-ESI/MS spectrum at *m/z* 452.2106 $[M+H]^+$ (calc. 452.2101). The IR spectrum showed the absorptions at 1652 and 1312 cm^{-1} for amide carbonyl and SO_2 groups, respectively. The ^1H and ^{13}C-NMR data (Table 1) showed signals for the functionalities of two carbonyls (δ_C 163.0 and 208.5), a *trans*-double bond and a 1,4-substituted phenyl, as well as five methyl groups (two oxygenated), six methylene groups (two oxygenated) and two oxygenated tertiary quaternary carbons. The above mentioned data together with the fact that the presence of SCAs[9] in *G. lucida* suggested that compound **1** was also a SCA.

Inspection of the 2D NMR spectra could allow the assignment of the structure of compound **1** (Figure 3). The observed ^1H–^1H COSY correlations (H-2/H-3, H_2-1′/H_2-2′, H-4′/H-5′ and H-7′/H-8′) and the HMBC cross peaks (H-2/C-1; N–CH_3/C-1 and C-1′; H_2-2′/C-3′, C-4′, C-8′; H-5′/C-6′, H-7′/C-6′ and SO_2–CH_3/C-3) could construct the fragment a (the *N*-methyl-*N*-phenethylacetamide moiety linked with SO_2–CH_3 at C-3 position). A geranyloxy derived fragment b was determined by the correlations of the ^1H–^1H COSY spectrum (H_2-1″/H-2″) and the HMBC spectrum (CH_3-10″/C-2″, C-3″ and C-4″; CH_3-8″/C-6″ and C-7″; CH_3-9″/C-7″ and C-8″; and CH_2-4″ and CH_2-6″/C-5″). The linkage of fragment a and b *via* the –C6′–O–C1″– bonds by the HMBC of H-1″/C-6′. The coupling constant of $J_{2,3}=14.9$ between H-2 and H-3 indicated that the double bond of C2–C3 was *trans*-configured (namely *E* configuration). The structure of compound **1** was therefore assigned as shown.

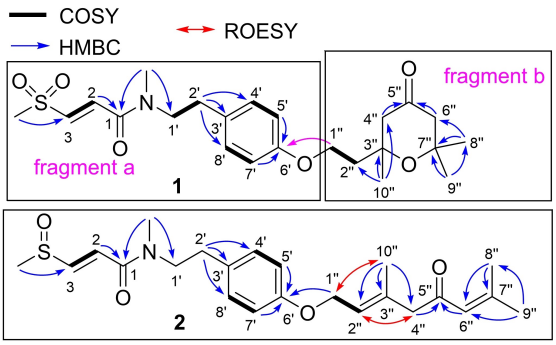

Figure 3. 2D NMR correlations analysis of compounds **1** and **2**.

The strong positive cotton effect around 195 nm in the ECD spectrum (Figure S1, *Supporting Information*), as well as the specific rotation value ($[\alpha]_D^{23}=-24.4$) indicated that compound **1** was the optically pure compound. However, the configuration at C-3″ in **1** remains unassigned.

Glylucidamide B (**2**) gave a molecular formula of $C_{23}H_{32}NO_4S$ based on the HR-ESI/MS spectrum at *m/z* 418.2053 $[M+H]^+$ (calc. 418.2047), showing a 16 mass unit less than that of methylgerambullone.[13] Comparison of its 1D NMR data (Table 1) with those of methylgerambullone indicated that they were structural analogs with the difference being the presence of CH_3–SO–CH– moiety in **2** instead of the CH_3–SO_2–CH– fragment in methylgerambullone.[13] This conclusion was further supported by the analysis of the 1D NMR data (Table 1) and 2D NMR spectrum (Figure 3). The structure of compound **2** was thus assigned as shown.

Nine known compounds were identified as glycocramide C (**3**), glycocramide A (**4**), glycocramide D (**5**),[14] glycopentamide L (**6**),[15] *p*-coumaroyltyramine (**7**),[16] *N*-benzoyltyramine methyl ether (**8**),[17] orberryamide B (**9**) and orberryamide B (**10**)[8] by comparison of their NMR and MS data with literatures.

Immunosuppressive activity assays

Due to the key role of Th17 in the pathogenesis of autoimmune diseases, we determined the effects of these isolated compounds on Th17 differentiation, with the exception of the previously evaluated compounds **9** and **10**.[8] As shown in Figure S2, compounds **1**–**8** significantly suppressed Th17 cell differentiation without cytotoxicity.

Table 1. ^{1}H (500 MHz) and ^{13}C (125 MHz) NMR data for compounds **1** and **2** in $CDCl_3$ (δ in ppm).

No.	1a[a] δ_H (Mult., *J* in Hz)	δ_C	1b[b] δ_H (Mult., *J* in Hz)	δ_C	2a[c] δ_H (Mult., *J* in Hz)	δ_C	2b[d] δ_H (Mult., *J* in Hz)	δ_C
1		163.0		162.4		163.9		163.2
2	6.88 (d, 14.9)	132.6	7.32 (d, 14.9)	133.4	6.80 (d, 14.3)	124.6	7.08 (d, 14.3)	125.2
3	6.99 (d, 14.9)	138.6	7.36 (d, 14.9)	139.6	7.29 (d, 14.3)	147.0	7.56 (d, 14.3)	148.1
1′	3.60 (t, 6.5)	52.4	3.64 (t, 6.5)	50.8	3.56–3.67 (m, 2H)	52.3	3.56–3.67 (m, 2H)	50.8
2′	2.81 (t, 6.5)	34.1	2.83 (t, 6.5)	32.6	2.78–2.82 (m, 2H)	34.3	2.78–2.82 (m, 2H)	32.7
3′		129.3		130.5		129.6		130.7
4′,8′	7.00 (d, 8.5)	130.2	7.11 (d, 8.5)	129.9	7.01 (d, 8.5)	130.1	7.09 (d, 8.5)	129.8
5′,7′	6.82 (d, 8.5)	115.1	6.84 (d, 8.5)	114.7	6.82 (d, 8.5)	115.1	6.82 (d, 8.5)	114.9
6′		157.9		157.5		157.8		157.5
1″	4.05–4.20 (m, 2H)	64.0	4.05–4.20 (m, 2H)	64.0	4.52 (d, 6.4)	64.7	4.54 (d, 6.4)	64.7
2″	1.99–2.03 (m, 2H)	43.1	1.99–2.03 (m, 2H)	43.1	5.56 (t, 6.4)	124.3	5.56 (t, 6.4)	124.5
3″		75.8		75.7		135.3		135.2
4″	2.71 (d, 15.6)	49.9	2.73 (d, 15.6)	49.9	3.12 s	55.0	3.12 s	55.1
	2.38 (d, 15.6)		2.40 (d, 15.6)					
5″		208.5		208.5		198.3		198.4
6″	2.42 s	51.5	2.42 s	51.5	6.09 s	122.9	6.09 s	122.9
7″		75.0		75.0		156.8		156.7
8″	1.31 s	30.8	1.31 s	30.8	2.12 s	20.9	2.12 s	20.9
9″	1.31 s	32.0	1.31 s	32.0	1.86 s	27.8	1.86 s	27.8
10″	1.34 (d, 4.4)	29.7	1.34 (d, 4.4)	29.8	1.72 s	17.1	1.72 s	17.1
S–CH_3	2.88 s	42.6	3.02 s	42.6	2.60 s	39.7	2.69 s	39.7
N–CH_3	3.05 s	34.4	2.99 s	36.7	2.99 s	34.5	3.00 s	36.6

[a]Amide configuration is *anti*-form (65 %). [b]Amide configuration is *syn*-form (35 %). [c]Amide configuration is *anti*-form (58 %). [d]Amide configuration is *syn*-form (42 %).

Since compounds **1**–**8** inhibited Th17 differentiation at 10 μM, we were interested in whether these compounds could inhibit Th17 differentiation at lower concentrations. As shown in Figure 4A, the results demonstrated that five of these compounds, including **1** and **3**–**6**, significantly inhibited Th17 cell differentiation at 5 μM. Remarkably, all of the compounds have no obvious cytotoxicity on the T cells up to 50 μM (Figure 4B), implying that the inhibitory effect of the compounds on Th17 cell differentiation did not result from its cytotoxicity.

Interestingly, we found that compounds **1** and **6** dose-dependently suppressed Th17 cell differentiation in a dose-dependent manner, and their IC_{50} values -were 0.36 and 1.30 μM, respectively (Figure 5A and 5E). However, compounds **3**–**5** did not exhibit dose-dependent suppressive effects on Th17 cells (Figure 5B–5D), indicating that **1** and **6** have potential as lead compounds for further investigation.

Due to the facts that the retinoic acid-related orphan receptor gamma t (RORγt) is the central transcriptional factor for Th17 cell differentiation *via* facilitating the expression of IL-17A, the lineage-defining cytokine of Th17 to maintain Th17 cell function,[18] we determined whether compounds **1** and **6** are the antagonists of RORγt resulting in the suppression on Th17 cells. As shown in Figure S2, none of these compounds could bind to RORγt ligand binding domain (LBD), implying that both of them inhibited Th17 differentiation is independent of RORγt.

Conclusions

In the present study, chemical investigation of *G. lucida* leaves led to the production of ten compounds, including six geranylated sulfur-containing amides (**1**–**6**), two amides (**7** and **8**) and two macrocyclic nonapeptides (**9** and **10**). Immunosuppressive activity assays revealed that compounds **1** and **6** significantly inhibited Th17 differentiation with IC_{50} values of 0.36 and 1.30 μM, respectively, and the effects are not associated with RORγt regulation. This is also the first reported of immunosuppressive chemicals from *G. lucida*. Our research data suggested that the geranylated sulfonyl amides may serve as lead compounds for the discovery of the drugs to treat autoimmune diseases via inhibition of Th17 cell differentiation.

Experimental Section

General Experimental Procedures

Optical rotations were obtained with a Autopol VI polarimeter at room temperature. UV spectra were measured with a Shimadzu UV-2401 A instrument. CD spectra were recorded on a Chirascan CD spectrometer. IR spectra were acquired using a Bruker Tensor-27 infrared spectrometer (KBr). The NMR spectra were obtained on Bruker AM-500 NMR spectrometers with TMS as an internal standard. Semi-preparative HPLC was performed on a Waters 1525 system with a 2487 UV detector using the column of YMC-Pack ODS–A (300×10 mm, S-5 μm). HR-ESI/MS spectra were got from an Agilent 1290 UPLC/6500 Q-TOF mass spectrometer. Silica gel (300–400 mesh, Qingdao Marine Chemical Co. Ltd), Sephadex LH-20 gel (40–70 μm, Amersham Pharmacia Biotech Ltd.), C18 reversed-phase silica gel (150–200 mesh, Merck Corp.), and MCI gel (CHP20/P120, 75–150 μm, Mitsubishi Chemical Industries Ltd.) were used for column chromatography (CC), and TLC was carried out with the GF254 plates (Qingdao Marine Chemical Co. Ltd.). All solvents used were analytical grade (Shanghai Chemical Reagents Co. Ltd.).

Plant materials

Glycosmis lucida leaves were collected from Mengla County of Yunnan Province (northern latitude: 21°56′9.15″, east longitude: 101°14′46.51″), China, in October 2020 and authenticated by

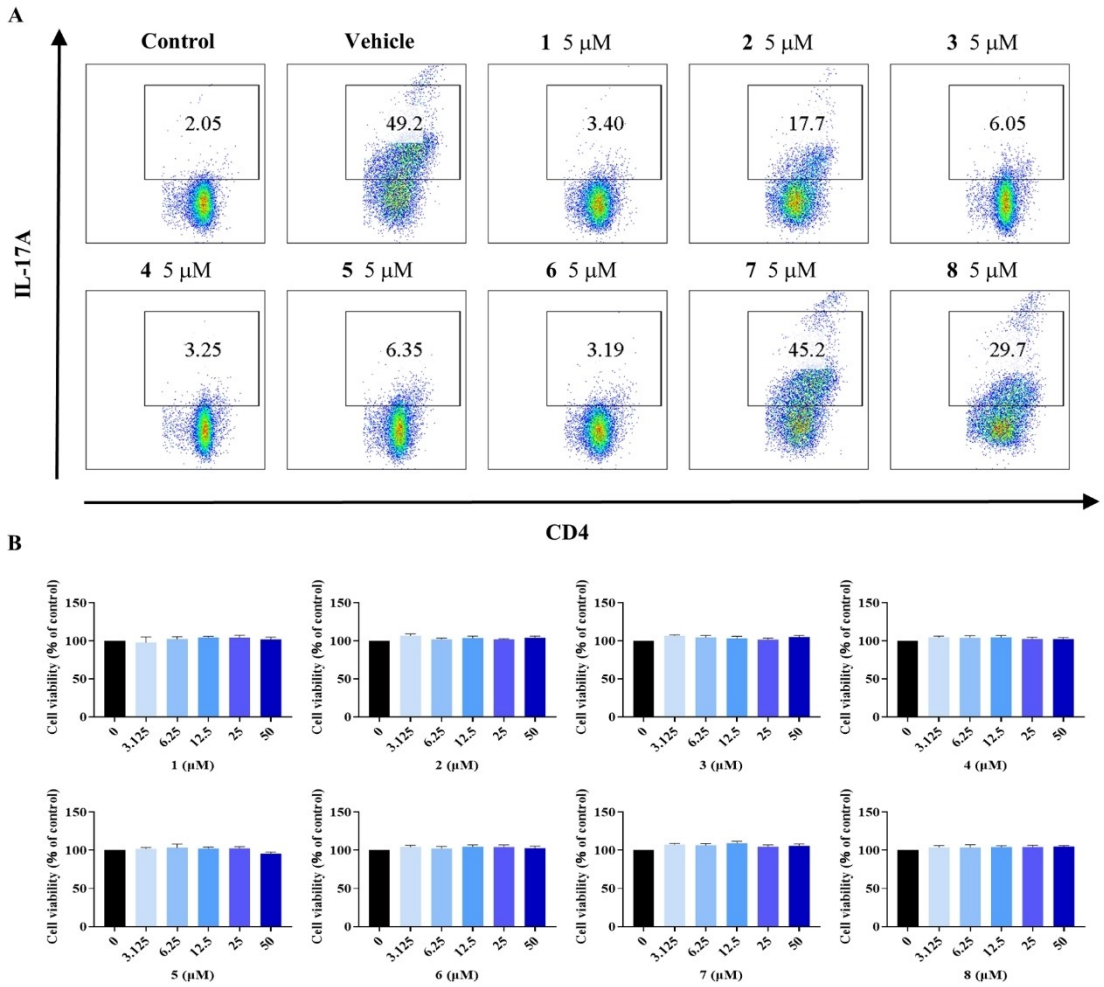

Figure 4. The effects of compounds **1**–**8** on Th17 cell differentiation at 5 μM (A) and their cytotoxicity on CD4+ T lymphocytes (B). The CD4+ T cells were prepared from the spleen of C57BL/6 mice and subjected to the Th17 cell differentiation condition. The effects of the compounds on the induction of IL-17, the lineage marker of Th17, were determined by flow cytometry. The cytotoxicity of compounds **1**–**8** on CD4+ T lymphocytes (B). CD4+ T cells were incubated with compounds at the indicated concentrations for 72 h, and the cell viability was determined by MTT assay. The results were obtained from three independent experiments.

professor You-Kai Xu (Xishuangbanna Tropical Botanical Garden (XTBG), Chinese Academy of Science (CAS)). A voucher specimen (HITBC 0026039) has been deposited in XTBG, CAS.

Extraction and isolation

Dried *G. lucida* leaves (5 kg) were ground to powder and extracted three times with 95% ethanol to give a total crude extract (200 g). The crude extracts were dissolved in water and partitioned with EtOAc to obtain an EtOAc-soluble fraction (75 g). To remove the pigment such as chlorophyll, the EtOAc-soluble fraction was subjected to MCI gel column chromatography (CC) eluted with a gradient MeOH/H_2O solvent system (v/v: 3/2, 7/3 and 4/1) to give three fractions F1–F3. The geranylated sulfonyl amides-rich fraction F2 was used for further chromatography and purification.

Firstly, fraction F2 was separated on a silica gel CC eluted with the gradient PE/Acetone (v/v: 5/1, 3/1, 2/1 and 1/1) together with TLC detection to give three major sub-fractions F2 A, F2B and F2 C. The fraction F2A was then further separated by Sephadex LH-20 gel CC eluted with MeOH to produce three small parts F2A–1, F2A–2 and F2A–3 after TLC analysis, of which HPLC treatment of the fraction F2A–2 with a gradient MeCN/H_2O solvent system (v/v: from 70% to 90%) yielded compound **2** (20 mg). Fraction F2A–3 was chromatographed on C18 reversed-phase silica gel CC (eluted with MeOH/H_2O from 3/2 to 4/1, v/v) to give three small sub-fractions F2A–3a, F2A–3b and F2A–3c with TLC detection. Fraction F2A–3b was purified by HPLC with 75% MeOH/H_2O solvent (v/v) to get compounds **1** (8 mg), **3** (60 mg) and **4** (80 mg). The similar treatment of F2A–3c by HPLC purification (eluted with 65% MeOH/H_2O, v/v) yielded compounds **5** (5 mg), **6** (10 mg) and **8** (7 mg). Fraction F2B was also initially separated on Sephadex LH-20 gel CC eluted by MeOH to give three fractions F2B–1, F2B–2 and F2B–3. Finally, compound **7** (10 mg) were obtained through the HPLC separation (eluted with MeOH/H_2O, from 60% to 80%, v/v).

Fraction F3 was initially separated on a Sephadex LH-20 gel CC, eluted with MeOH, to afford four fractions F3A–F3C, of which F3B contained mainly compounds **9** and **10**. Further purification of the fraction F3B by HPLC (eluted with 60% MeCN/H_2O, v/v) to give compounds **9** (100 mg) and **10** (10 mg).

Glylucidamide A (**1**): Colorless gum; $[\alpha]_D^{23} = -24.4$ ($c = 0.07$, MeOH); UV (MeOH) λ_{max} (log ε) 203 (4.53), 224 (4.40), 273 (3.90) nm; IR (KBr) ν_{max} 2978, 2935, 1714, 1651, 1616, 1512, 1406, 1314, 1247, 1137,

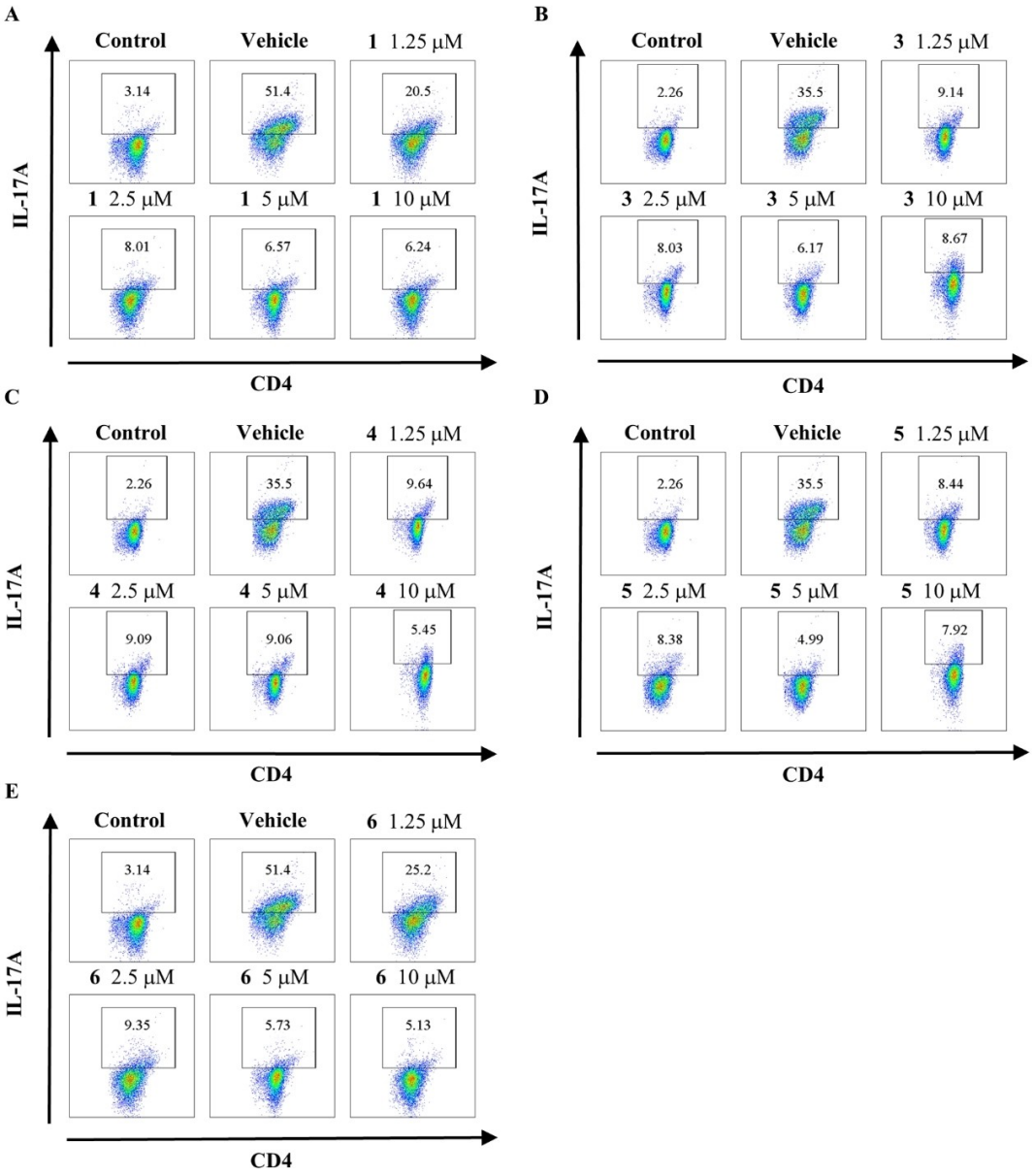

Figure 5. The effects of compounds **1** and **3**–**6** on Th17 cell differentiation from 1.25 to 10 μM (A–E). The CD4+ T cells were prepared from the spleen of C57BL/6 mice and subjected to the Th17 cell differentiation condition, and the effects of compounds on Th17 were determined by flow cytometry. The results were obtained from three independent experiments.

1021, 972 cm^{-1}; ^{1}H and ^{13}C-NMR: Table 1; (+)-HR-ESI/MS *m/z* 452.2106 $[M+H]^+$ (calc. for $C_{23}H_{34}NO_6S$, 452.2101).

Glylucidamide B (**2**): Colorless gum; UV (MeOH) λ_{max} (log ε) 202 (4.46), 227 (4.32), 255 (4.25) nm; IR (KBr) ν_{max} 2923, 1638, 1611, 1511, 1440, 1402, 1302, 1239, 1181, 1116, 1066, 958 cm^{-1}; ^{1}H and ^{13}C-NMR: Table 1; (+)-HR-ESI/MS *m/z* 418.2053 $[M+H]^+$ (calc. for $C_{23}H_{32}NO_4S$, 418.2047).

$CD4^+$ T cell purification and Th17 cell differentiation

The splenic $CD4^+$ T cells were prepared by magnetic beads from C57BL/6 mice (Miltenyi Biotec, Cologne, Germany) and cells were induced into Th17 cell subsets according to previous description.[19] The purified $CD4^+$ T cells were treated with or without indicated compounds for 72 h, and restimulated with 50 ng/mL of PMA, 1 μg/mL of ionomycin, and 1 μg/mL of brefeldin A for another 5 h before intracellular staining.

Flow cytometric analysis

For detecting Th17 cell differentiation, PerCP/Cy5.5 anti-mouse CD4 was applied to stain the surface marker of cells. After the cells were permeabilized, PE anti-mouse IL-17 A was used to stain intracellular cytokines. After washing three times with PBS, the expression levels of these cytokines were determined by BD FACSAria III (BD Bioscience) and analyzed by FlowJo.

Cell viability

The splenic $CD4^+$ T cells were isolated from C57BL/6 mice and were seeded at a density of 1×10^5 in 96-well plates followed by exposed to the indicated compounds at different concentrations or solvent control for 72 h. Subsequently, 10 μL 3-(4,5-dimethylthiazol-2-yl)-3,5-phenytetrazoliumromide (MTT) was added to each well for 4 h followed by the addition of 100 μL solubilization buffer (10% SDS in 0.01 mol/L HCl) for overnight incubation. The optical density (OD) was measured at 570 nm by a plate reader (Tecan, Männedorf, Switzerland).

Binding affinity assay

The Bio-layer interferometry (BLI) assays were conducted on an Octet RED96 (FortéBio, United States) instrument. A shake speed of 1000 rpm and plate temperature of 24 °C were applied to all runs. Phosphate buffer solution containing 2% DMSO (PBS + 2% DMSO) was used as a kinetics buffer. To prepare recombinant human RORγt-LBD protein bound test probes, HIS1 K biosensor (HIS) optic fiber probes were run at baseline in PBS for 120 s, loaded in 200 μL of RORγt-LBD-HIS solution at 40 μg/mL for 600 s, run at baseline again in PBS for 60 s, and stored at 4 °C dipped in PBS. For binding kinetics assays, a serial dilution of six concentrations of up to seven drugs dissolved in PBS was added to a black polypropylene 96-well microplate (Greiner Bio-one, Frickenhausen, Germany) with PBS filling the rest of the wells. One row was left as PBS-only negative control. Each well contains a total volume of 200 μL. An assay cycle consists of 120 s of baseline incubation in PBS followed by 120s of association in compound solution followed by 120s of dissociation in PBS, and it was repeated for every concentration with both an RBD-loaded and a blank probe. The results were analyzed by FortéBio Data Analysis software version 9.0.

Author Contributions

K. L. Ji: performed the experiments for the isolation, structure elucidation, supervised the research work, and prepared and revised the manuscript. Y. Q. Tang: performed the experiments for bioassays, prepared the manuscript. Z. Y. Guo: performed the experiments for bioassays, prepared the manuscript. P. Sun: contributed to part of the structure determination; J. M. Lu: performed the medicinal plant collection. M. Y. Dai: performed the experiments data collection and analysis. Ting Li: supervised the research work and revised the manuscript.

Acknowledgements

This study was financially supported by Yunnan Fundamental Research Projects (No.202101AU070148 and No.202101AT070055) and National Natural Science Foundation of China (No. 82104268). Authors also acknowledge the Institutional Central for Shared Technologies and Facilities of XTBG, CAS for the technical supports.

Conflict of Interests

The authors declare no conflict of interest.

Data Availability Statement

The data that support the findings of this study are available from the corresponding author upon reasonable request.

Keywords: *Glycosmis lucida* · geranylated sulfonyl amides · glylucidamides · Th17 differentiation · RORγt

[1] H. Park, Z. Li, X. O. Yang, S. H. Chang, R. Nurieva, Y. H. Wang, Y. Wang, L. Hood, Z. Zhu, Q. Tian, C. Dong, *Nat. Immunol.* **2005**, *6*, 1133–1141.
[2] L. E. Harrington, R. D. Hatton, P. R. Mangan, H. Turner, T. Murphy, K. M. Murphy, C. T. Weaver, *Nat. Immunol.* **2005**, *6*, 1123–1132.
[3] D. L. P. Baeten, V. K. Kuchroo, *Nat. Med.* **2013**, *19*, 824–825.
[4] K. Yasuda, Y. Takeuchi, K. Hirota, *Semin. Immunopathol.* **2019**, *41*, 283–297.
[5] Flora of China Editorial Committee, In *Flora of China*; *Science Press*: Beijing, **1997**; Vol. 43, p 117–126.
[6] P K. Teja, P. Patel, D. Bhavsar, C. Bindusri, K. Jadhav, S. K. Chauthe, *Phytochemistry* **2021**, *190*, 112865.
[7] Z. F. Geng, K. Yang, S. S. Guo, W. J. Zhang, C. X. You, J. Y. Liang, Z. W. Deng, S. S. Du *Magn. Reson. Chem.* **2016**, *54*, 994–997.
[8] K. L. Ji, Y. Y. Fan, H. H. Kuok, Q. F. Liu, T. Li, J. M. Yue, *CCS. Chem.* **2021**, *3*, 844–858.
[9] K. Yang, S. S. Guo, Z. F. Geng, C. X. You, W. J. Zhang, Y. P. Li, C. F. Wang, S. S. Du, Z. W. Deng, *Ind. Crops Prod.* **2015**, *74*, 628–634.
[10] S. S. Guo, W. J. Zhang, K. Yang, J. Y. Liang, C. X. You, C. F. Wang, Y. P. Li, Z. F. Geng, Z. W. Deng, S. S. Du, *Nat. Prod. Res.* **2017**, *31*, 1201–1204.
[11] Z. F. Geng, K. Yang, Y. P. Li, S. S. Guo, C. X. You, W. J. Zhang, Z. Zhang, S. S. Du, *Nat. Prod. Res.* **2017**, *31*, 791–796.
[12] H. Greger, O. Hofer, H. Kählig, G. Wurz, *Tetrahedron* **1992**, *48*, 1209–1218.
[13] H. Greger, O. Hofer, G. Zechner, F. Hadacek, G. Wurz, *Phytochemistry* **1994**, *37*, 1305–1310.
[14] S. Y. Wu, Z. M. Chen, Q. Zhou, G. L. Huang, Z. L. Zhou, M. Bai, *Fitoterapia* **2023**, *165*, 105418.
[15] H. Nian, H. Xiong, F. Zhong, H. Teng, H. Teng, Y. Chen, G. Yang, *Fitoterapia* **2020**, *144*, 104693.
[16] J. K. Reinhardt, A. M. Zimmermann-Klemd, O. Danton, M. Smieško, C. Gründemann, M. Hamburger, *J. Nat. Prod.* **2020**, *83*, 3012–3020.
[17] X. M. Niu, S. H. Li, L. Y. Peng, Z. W. Lin, G. X. Rao, H. D. Sun, *'J. Asian Nat. Prod. Res.* **2001**, *3*, 299–311.
[18] R. Kumar, A. L. Theiss, K. Venuprasad, *Trends Immunol.* **2021**, *42*, 1037–1050.
[19] Z. N. Yang, X. S. Yang, *Mol. Pharmaceutics* **2019**, *16*, 798–807.

Manuscript received: March 13, 2023
Accepted manuscript online: May 10, 2023
Version of record online: May 22, 2023